(6) Fluorine Hfsc's. Comparing the β-fluorine hfsc's of $C(CF_3)_3$ with its hydrocarbon counterpart, $C(CH_3)_3$ (A_H^β = 22.93 at −113 °C), we find that A_F^β is smaller than A_H^β. This is in spite of the fact that their respective equilibrium geometries favor a larger A_F^β. The same trend is observed for perfluoro-*tert*-pentyl radicals: $A_F^\beta(CF_3)$ = 18.6 and $A_H^\beta(CH_3)$ = 22.77.

It is generally accepted that β atoms obtain spin density mostly via hyperconjugation. The fact that $A_F^\beta < A_H^\beta$ can thus be explained by the relative energies of CF_3 and CH_3 group orbitals to the unpaired electron orbital. The CF_3 group orbital of π symmetry which interacts with the unpaired electron orbital will be lowered in energy by replacement of fluorine for hydrogen and the hyperconjugation will therefore be less effective. This kind of phenomena was also noticed in the dramatic reduction of A_H^β in the methylene group of hexafluorocyclohexadienyl radical[12] and was explained in the same way. Stock and Wasieluski[21] have also pointed out this reduction of β-proton hfsc's in β-fluorinated radicals. A closely related argument has been forwarded to explain the difference in magnitude of the A_F^β between hexafluoroacetone anion and bis(trifluoromethyl) nitroxide.[22,23]

Chen et al.[15] observed that B_F and B_H for the β interaction ($A_\beta = A + B\cos^2\theta$) are not constant for the fluorinated ethyl radicals and decrease with the extent of β-fluorine substitution for hydrogen, such as in Chart I. This reduction would be expected qualitatively on the basis of the above arguments. The reduction in hyperconjugation with the CF_3 group filled orbitals as a result of their lowering will reduce the charge density on the trigonal carbon compared to the CH_3 analogue. This in turn should result in a more carbonium-ion like structure and therefore a more planar one for the perfluoro-*tert*-butyl radical. This result together with the σ^*-π^* crossover phenomena observed in fluorinated benzene anions[11] shows that fluorine substitution for hydrogen affects energy levels dramatically and is an important factor in explaining fluorine hfsc's in general.

Chart I

	CH_3CH_2	CH_2FCH_2	CF_2HCH_2	CF_3CH_2
B_H, G	51	46	41	
B_F, G		106	92	59

Acknowledgment. We acknowledge the donors of the Petroleum Research Fund, administered by the American Chemical Society, for support of this research, and the University of Connecticut Computer Center for a grant of computer time.

References and Notes

(1) C. Hesse and J. Roncin, *Mol. Phys.*, **19**, 803 (1970).
(2) M. C. R. Symons, *Mol. Phys.*, **24**, 461 (1972).
(3) M. C. R. Symons, *Tetrahedron Lett.*, 207 (1973).
(4) D. E. Wood, L. F. Williams, R. F. Sprecher, and W. A. Lathan, *J. Am. Chem. Soc.*, **94**, 6241 (1972).
(5) D. E. Wood and R. F. Sprecher, *Mol. Phys.*, **26**, 1311 (1973).
(6) P. J. Krusic and P. Meakin, *J. Am. Chem. Soc.*, **98**, 228 (1976).
(7) J. B. Lisle, L. F. Williams, and D. E. Wood, *J. Am. Chem. Soc.*, **98**, 227 (1976).
(8) T. Koenig, T. Balle, and W. Snell, *J. Am. Chem. Soc.*, **97**, 662 (1975).
(9) (a) R. V. Lloyd, D. E. Wood, and M. T. Rogers, *J. Am. Chem. Soc.*, **96**, 7130 (1974); (b) R. V. Lloyd and D. E. Wood, *ibid.*, **97**, 5986 (1975).
(10) R. V. Lloyd and M. T. Rogers, *J. Am. Chem. Soc.*, **95**, 1512 (1973).
(11) M. B. Yim and D. E. Wood, *J. Am. Chem. Soc.*, **98**, 2053 (1976).
(12) M. B. Yim and D. E. Wood, *J. Am. Chem. Soc.*, **97**, 1004 (1975).
(13) N. J. Maraschin and R. J. Lagow, *Inorg. Chem.*, **12**, 1458 (1973).
(14) R. W. Fessenden and R. H. Schuler, *J. Chem. Phys.*, **43**, 2704 (1965).
(15) K. S. Chen, P. J. Krusic, P. Meakin, and J. K. Kochi, *J. Phys. Chem.*, **78**, 2041 (1974).
(16) J. A. Pople, D. L. Beveridge, and P. A. Dobosh, *J. Am. Chem. Soc.*, **90**, 7142 (1968); J. A. Pople and D. L. Beveridge, "Approximate Molecular Orbital Theory", McGraw-Hill, New York, N.Y., 1970.
(17) P. Meakin and P. J. Krusic, *J. Am. Chem. Soc.*, **95**, 8185 (1973).
(18) R. W. Fessenden and R. H. Schuler, *J. Chem. Phys.*, **39**, 2147 (1963).
(19) J. Lin and F. Williams, *J. Phys. Chem.*, **72**, 3707 (1968).
(20) J. K. Kochi and P. J. Krusic, *Chem. Soc., Spec. Publ.*, **No. 24** (1970).
(21) L. M. Stock and M. R. Wasieluski, *J. Am. Chem. Soc.*, **97**, 5620 (1975).
(22) W. R. Knolle and J. R. Bolton, *J. Am. Chem. Soc.*, **93**, 3337 (1971).
(23) K. Morokuma, *J. Am. Chem. Soc.*, **91**, 5412 (1969).

Single Crystal EPR, Zero-Field ODMR, and Phosphorescence Studies of the T_1 State of Coumarin

Edward T. Harrigan, Asok Chakrabarti, and Noboru Hirota*

Contribution from the Department of Chemistry, State University of New York at Stony Brook, Stony Brook, New York 11794. *Received September 2, 1975*

Abstract: Single-crystal EPR, zero-field ODMR, phosphorescence excitation, and emission studies of the T_1 state of coumarin were made using durene and 1,4-dibromobenzene (DBB) host. It was shown that $D = 0.0984\ cm^{-1}$ and $|E| = 0.0414\ cm^{-1}$ in durene host when the out-of-plane axis is taken as the z axis. Hyperfine splittings observed in the x, y, and z axis spectra in durene host indicate about 0.5 spin density on the -C=C- group of the pyrone moiety. The phosphorescence excitation spectrum shows that the $^3n\pi^*$ state is far above the T_1 ($^3\pi\pi^*$) state and the location of the $^1n\pi^*$ state is likely to be close to that of the lowest $^1\pi\pi^*$ state. It was found that $k_x > k_y \gg k_z$ as in other $^3\pi\pi^*$ aromatic carbonyls, but k_x^r and k_y^r are strongly dependent on the vibrational bands. At 0–0 and 0–1628 cm^{-1} bands, $k_y^r > k_x^r$ indicating the importance of the $^1\sigma\pi^*$ ($^1\pi\sigma^*$) state mixing in the radiative process contrary to the cases of many other $^3\pi\pi^*$ aromatic carbonyls. Vibronic band dependence of $(k_x^r - k_y^r)$ was studied by means of the rapid passage microwave modulated phosphorescence spectrum and the microwave induced delayed phosphorescence technique. Observed results are discussed in terms of the possible mechanisms of radiative and nonradiative decay. The external heavy-atom effect in DBB host is briefly described.

I. Introduction

The photochemical and photobiological behavior of coumarin have attracted considerable attention in recent years.[1-8] It is considered that the lowest excited triplet state plays an important role in these processes. In particular, dimerization and addition at the ethylenic double bond in the pyron moiety appear to be related to the large spin densities there.[5] Cou-

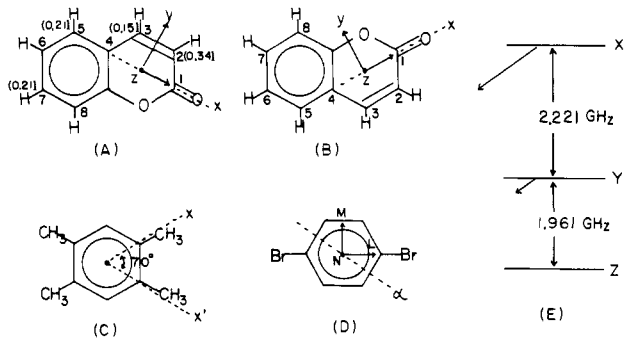

Figure 1. Molecular structures; the axis systems of coumarin in durene and 1,4-dibromobenzene (DBB) and the spin sublevel energy level scheme. (A) and (B) indicate two different ways in which coumarin replaces durene. Estimated spin densities are given by the numbers in parentheses in (A).

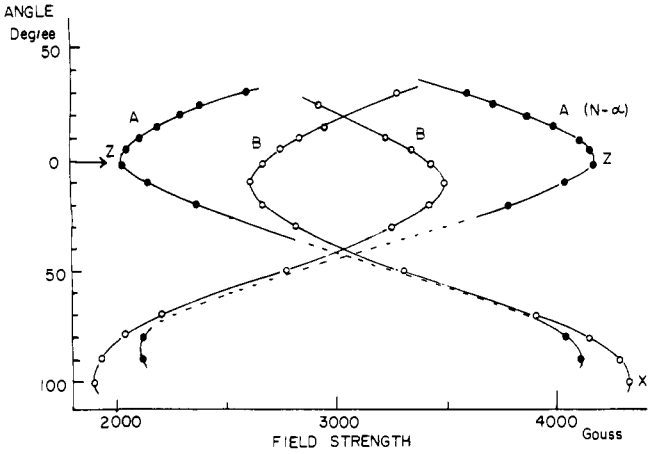

Figure 2. Angular dependence of the EPR signals of coumarin in DBB host. Crystal was mounted so that **H** rotates approximately within N-α plane of one type of coumarin molecule (A) when the sample holder was rotated. (●) Signal from the A type molecule. (○) Signal from the other type molecule. z and x indicate the approximately z and x axes peaks, respectively. → indicate the orientation at which the molecular plane of the A type molecule is approximately perpendicular to **H**.

marin is also considered as an aromatic carbonyl, but its lowest $^3\pi\pi^*$ state does not have nearby $^3n\pi^*$ and $^1n\pi^*$ states as in other $^3\pi\pi^*$ aromatic carbonyls. Comparison of its property with the known properties of other aromatic carbonyls[9-11] and enones[13,14] would be useful. Therefore, it seems desirable to obtain detailed information about the magnetic and dynamic properties of the T_1 state of coumarin.

There have been several spectroscopic[4-8] and magnetic resonance[15] studies of coumarin in recent years. However, these studies were made using a rigid glass matrix at 77 K. The information obtained from such studies has been limited considerably.

In our preliminary ODMR studies of coumarin we have noted that the radiative properties of coumarin are quite different from those of the other $^3\pi\pi^*$ aromatic carbonyls.[16] We also noted that 1,4-dibromobenzene and durene are good hosts for single-crystal EPR studies.[17] Accordingly, we have made detailed EPR, zero-field ODMR and phosphorescence studies of coumarin using mixed and pure single crystal systems in the hope of obtaining detailed information about the nature of the T_1 state.

II. Experimental Section

1. Sample Preparations. Mixed single crystals of coumarin guest in durene and 1,4-dibromobenzene (DBB) host were prepared by the standard Bridgman method. The guest concentrations of the initial melts were about 1% by weight, but the actual guest concentrations are considered to be much less. Host and guest materials obtained from Aldrich Chemical Co. were purified by recrystallization followed by extensive zone refining. The molecular structures, axis directions, and numbering systems of the guest and host molecules are given in Figure 1.

2. Single-Crystal EPR Study. Single crystal EPR studies were made at 77 K using a Varian V-4502 spectrometer in the case of DBB host and a E-12 spectrometer in the case of durene host. The experimental procedure for the DBB host systems was the same as described in previous papers.[18,19] In case of durene host we followed the procedure described by Hutchison and Mangum.[20] However, the crystal mounting was made by conoscopic observation with a polarizing microscope.

3. Single-Crystal Phosphorescence Emission and Excitation Spectra. Phosphorescence spectra of coumarin in durene, and DBB host and coumarin X traps were obtained at 1.5 K using our zero-field ODMR setup described elsewhere.[21] The phosphorescence excitation spectra[22,23] were taken at 4.2 K by modifying our zero-field ODMR setup to use an Engis 60-cm monochromator as the excitation monochromator analyzing the output of an Osram 1000w xenon lamp. The total phosphorescence emission of the sample was chopped at 720 s^{-1} and detected with an EMI 6256 B PM tube and a PAR HR-8 lock-in amplifier.

4. Zero-Field ODMR Experiments. (a) Microwave Induced Delayed Phosphorescence (MIDP) Experiments. The total decay rate (k_i), relative radiative decay rate (k_i^r), and populating rate (p_i) of each spin sublevel were determined at 1.2 K by the standard MIDP technique.[24,25] k_i^r was determined at several selected vibrational bands.

(b) Microwave Modulated Phosphorescence Spectra. In order to clarify the radiative mechanism of coumarin we have investigated the changes produced in the phosphorescence spectra by the microwave transitions among triplet spin sublevels. The commonly used method for doing this is the AM-PMDR (amplitude modulated phosphorescence microwave double resonance) method.[26-28] However, here we have detected changes in emission caused by the rapid sweep of microwave through resonance frequency (rapid passage) in order to obtain better S/N ratios in our systems. The microwave was repetitively swept at the rate of 3 s^{-1} and the changes produced in the phorescence were detected with a lock-in amplifier while the monochromator was scanned. The intensity of the signal (I) is given by[29]

$$I = A(k_i^r - k_j^r)(n_j - n_i) \tag{1}$$

where A is a proportionality constant which depends on the sample and the apparatus. Here k_i^r is the radiative decay rate constant of the ith sublevel and n_i is the steady state population of the ith level. In our experiment on coumarin in durene $n_y > n_x$. Therefore, the sign of I gives the relative values of k_x^r and k_y^r at different vibronic bands.

III. Results and Analysis

1. High-Field EPR Results. The observed EPR signals are explained in terms of the usual spin Hamiltonian[20,30]

$$\mathcal{H} = \beta \mathbf{H} \cdot \tilde{g} \cdot \mathbf{S} + DS_z^2 + E(S_x^2 - S_y^2) + \sum_i \mathbf{S} \cdot A_i \cdot \mathbf{I}_i \tag{2}$$

where A_i is the hyperfine tensor for the nucleus i.

DBB crystal is monoclinic with two molecules per unit cell.[31] The mixed crystal of DBB containing coumarin gives two sets of EPR signals coming from coumarin molecules occupying two translationally inequivalent sites. In Figure 2 angular dependence curves of the EPR signals are given for the case when the crystal was mounted so that the applied magnetic field (**H**) rotates approximately within the N-α plane (Figure 1) of one of the translationally inequivalent molecules.[32] In this crystal mounting **H** is approximately perpendicular to the molecular plane of this type molecule at a sample rotation angle of about 0°. At this orientation we obtain the stationary point signals at 2035 and 4165 G. Since the coumarin molecule is expected to replace DBB with their molecular planes approximately parallel to each other, these peaks are assigned as the out-of-plane (z axis) peak. When we mount the crystal so that **H** rotates within the molecular plane of one type of DBB

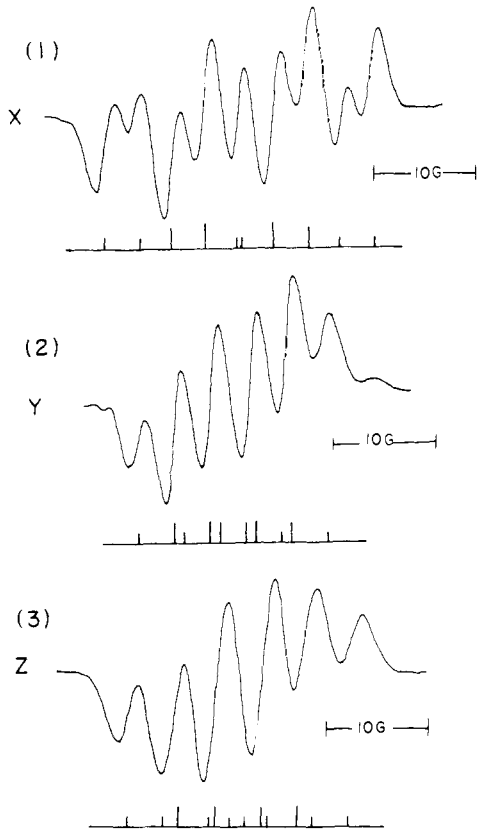

Figure 3. Hyperfine structures of the x, y, and z axes spectra obtained in durene host. Stick diagrams indicate the spectra obtained from the assignment given in section III.1: (1) x-axis spectrum, (2) y-axis spectrum, (3) z-axis spectrum.

molecule, we found the stationary point signals at 1910, 4325 and 2875, 3190 G. These peaks are assigned as the in-plane axis peaks (x and y). $D = 0.1003\ cm^{-1}$ and $E = -0.0425\ cm^{-1}$ determined from these measurements are in good agreement with those determined by the zero-field ODMR experiments.

If we assign the z sublevel to be the bottom one as in all other $^3\pi\pi^*$ molecules,[33] these observations unambiguously show that $|E_x - E_y| > |E_z - E_y|$ as shown in Figure 1B. Then D is smaller than $|3E|$ in the axis system adapted here. The ZFS determined in this axis system is quite different from that determined by Graber et al.,[15] but D and $|E|$ become similar to those obtained by them if we interchange the x and z axes.

The above assignment is entirely consistent with the results obtained by using durene host. In the case of durene host there are two in-plane axis signals coming from coumarin molecules which replace durene in two ways (A and B in Figure 1) with their x axes approximately along two different C-CH_3 direction of durene (x and x' in Figure 1C). The angle between the x directions of the two in-plane signals is 70 ± 3° which is close to the angle between the two C-CH_3 directions of a durene molecule.

The signals obtained in durene host show well resolved hyperfine patterns as shown in Figure 3. The y and z axis spectra consist of six peaks with nearly equal separations. If we assume that the coumarin rings are hexagonal and the directions of the x and y axes are parallel and perpendicular to the C=O directions, **H** is 60 and 30° away respectively from the C-H directions of the protons at 2, 3, 5, 7, and 8 positions at the x and y stationary points. When the direction of **H** is θ away from the C-H direction, the hfsc for a C-H proton interacting with a unit spin density on the adjacent carbon is given by,[20,34]

$$A(\theta) = [A_x^2 \sin^2\theta + A_y^2 \cos^2\theta]^{1/2} \quad (3)$$

Using $A_x = 102.1$ MHz and $A_y = 32.2$ MHz determined by using triplet state naphthalene,[35] we obtain $A(60°) = 90.1$ MHz and $A(30°) = 58.4$ MHz.

If the hfsc's are mainly due to the protons at 2, 3, 5, 7, and 8 positions, and the above assumptions are correct, the ratio of the total spread of the x and y axis peaks should be approximately $A(60°)/A(30°) = 1.54$. The total spreads of the x and y axis spectra observed are 28.0 and 18.0 G, respectively, giving the ratio 1.44. In fact, $A(57.8°)/A(32.2°)$ gives 1.44. This result strongly indicates that the directions of the x and y axis are indeed close to parallel and perpendicular to the C=O direction. This conclusion is in agreement with the prediction based on the calculation by Zuclich.[36]

Because of poor molecular symmetry it is difficult to make an unambiguous assignment of hfs and an accurate determination of spin distribution. Here we attempt to make a tentative assignment which is compatible with the observed spectra. The six-line pattern of the z axis spectrum indicates about 4.5 G splittings from three protons and a 8-9 G splitting from one proton. However, the intensity ratio indicates that the splittings from three protons are not identical. We first assume 8.0, 5.0 (two protons), and 3.5 G splittings for the z-axis spectrum. This assignment produces six groups of lines as indicated by the stick diagram in Figure 3. We analyze the other spectra in a similar way. The stick diagrams obtained from our assignment are shown together with the observed spectra. The assigned splittings are shown below:

Z, G	X, G	Y, G
8.0	10.0 (10.9)	7.0 (7.0)
5.0 (two protons)	6.5 (6.5)	4.0 (4.4)
3.5	3.0 (5.4)	3.0 (3.0)

Starting from the assigned splittings of the z-axis spectrum and the known proton hyperfine tensors at each orientation we can predict the splittings expected for each axis spectrum. They are given in the parenthesis above and are compared with the values deduced from the observed spectra. Excluding the smallest splitting of the x-axis spectrum the agreements are reasonably good. However, the above analysis is crude in several ways. First, we assumed hexagonal structures for the coumarin rings. Second, the x and y axes were assumed to be exactly parallel and perpendicular to the C=O direction. Third, only hyperfine interaction between the proton and the spin density at the nearest carbon atom was considered. These three assumptions are all not strictly correct. Considering these approximations, we think that our assignment explains the observed spectra reasonably well.

2. Phosphorescence Emission and Excitation Spectra. The phosphorescence spectrum of coumarin in durene host crystal at 1.2 K is shown in Figure 4. It is seen that each vibronic band consists of a doublet. Such doublet structures have often been found in durene host.[37,38] As already noted in the low-resolution phosphorescence spectrum, the strong vibronic bands are the 0-0 and the 0-1628 cm^{-1} bands.[5,8] However, we can identify a number of relatively weak bands which have not been reported previously. The vibrational analysis is given in Table I. These frequencies may be compared with the infrared data of ground state coumarin.[39,40] In Figure 4 phosphorescence excitation spectra are also shown. The excitation spectrum of coumarin crystal shows a weak absorption starting at 22 055 cm^{-1}, which is 115 cm^{-1} higher than the 0-0 of the trap phosphorescence spectrum of the coumarin crystal and is considered as the origin of the $^3\pi\pi^*$ state. This origin is blue shifted by 500 cm^{-1} from the 0-0 of the phosphorescence in durene host. A strong absorption starts at about 27 900 cm^{-1} which we tentatively assign as the origin of the $^3n\pi^*$ state. A very strong absorption starts at 28 500 cm^{-1} which can be due to either the $^1n\pi^*$ or $^1\pi\pi^*$ state. The origin of the fluorescence spectrum agrees with the beginning of this absorption and the

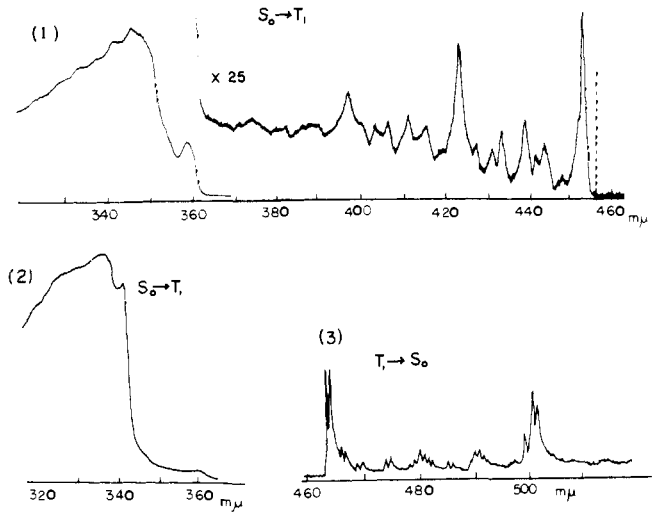

Figure 4. Phosphorescence excitation and emission spectrum. (1) Phosphorescence excitation spectrum of pure coumarin crystal at 1.5 K. Vertical dotted line indicates the origin of the trap phosphorescence. (2) Phosphorescence exictation spectrum of coumarin in durene. (3) Phosphorescnce spectrum of coumarin in durene at 1.5 K.

$^1\pi\pi^*$ assignment is favored as discussed by Mantulin and Song.[8] These authors suggested that the $^1\pi\pi^*$ ($^1B_1$) state is lower than the $^1n\pi^*$ state. Our result on coumarin crystal seems to be in agreement with their conclusion. The excitation spectrum of coumarin in durene crystal shows a very weak peak starting at 27 900 cm^{-1} which is assigned as the 0-0 of the $S_0 \rightarrow {}^3n\pi^*$ absorption. A strong absorption starts at 29 150 cm^{-1}. In the ordinary aromatic carbonyls the energy separation between $^3n\pi^*$ and $^1n\pi^*$ states is normally 1000-2000 cm^{-1}.[11-13] If this is also true in coumarin and the origin of the $^3n\pi^*$ state is located at 27 900 cm^{-1}, the origin of the $^1n\pi^*$ state should be at 29 400 ± 500 cm^{-1}. This is very close to the 0-0 band of the strong absorption. Therefore, the location of the $^1n\pi^*$ state is likely to be close to that of the lowest $^1\pi\pi^*$ ($^1B_1$) state, although it may be higher than the lowest $^1\pi\pi^*$ state.

The excitation spectrum of the coumarin crystal shows well-resolved vibronic bands. Vibrational frequencies are given in Table II. The main progression consists of a 1550-cm^{-1} vibration which is considered to be the -C=C- stretching frequency in the T_1 state.

3. Zero-Field ODMR Results. The total decay rates, relative radiative decay rates, and populating rates from spin sublevels determined by the standard MIDP method are tabulated in Table III. Representative decay curves obtained at the different vibronic bands are given in Figure 5.

Despite the poor molecular symmetry, it is found that $k_x \gg k_y \gg k_z$ and k_x^r and k_y^r are strongly dependent on the vibronic bands. The MIDP experiments monitored at the different vibronic bands show that $(k_x^r - k_y^r)$ is negative at the 0-0 and 0-1628 cm^{-1} bands, but positive at the 0-691 and 0-836 cm^{-1} bands. The decay curves shown in Figure 5 show that the emission at the 0-0 band comes dominantly from the y sublevel but at the 0-836 cm^{-1} bands the x sublevel emission dominates.

The vibronic band dependence of k_i^r is most clearly seen from the microwave modulated phosphorescence spectrum shown in Figure 6. The spectrum shows that $(k_x^r - k_y^r) < 0$ at the 0-0, 0-489, 0-1153, 0-1186, 0-1560, and 0-1628 cm^{-1} bands. These vibrations are considered as a′ vibrations. Signals are particularly strong at the 0-0 and the 0-1628 cm^{-1} bands. The 1628 cm^{-1} band is considered to be due to the -C=C- stretching of the pyrone group.[5] Therefore, this observation is in agreement with the observation that the y sublevel emission of the $^3\pi\pi^*$ aromatic carbonyl is usually strong at the 0-0 and the -C=C- stretching bands.[12] On the other hand, $(k_x^r - k_y^r) > 0$ was found at the 0-127, 0-262, 0-691, 0-836, and 0-990 cm^{-1} bands indicating that the origin of the x sublevel emission is mainly vibronic-spin orbit. These vibrations are

Table I. Vibrational Frequencies of the Phosphorescence Spectrum and the Emitting Sublevel

ν, cm^{-1}	$\Delta\omega$, cm^{-1}	Main emitting sublevel	Assignment
21 587		y	
21 460	127	x	a″
21 325	262	x	a″
21 098	489	y	a′
20 896	691	x	a″
20 821	766	y	a′
20 751	836	x	a″
20 597	990	x	a″
20 434	1153	y	a′
20 401	1186	y	a′
20 322	1265	y	a′
20 092	1495		
20 027	1560	y	a′
19 959	1628	y	a′

Table II. Vibrational Frequencies of the Excitation Spectrum

ν cm^{-1}	$\Delta\nu$, cm^{-1}	Intensity[a]
22 055		s
22 325	270	w
22 527	472	m
22 625	570	w
22 761	707	m
23 054	999	m
23 190	1135	m
23 390	1335	w
23 605	1550	s
23 866	1550 + 261	w
24 055	1550 + 460	m
24 287	1550 + 682	m
24 592	1550 + 987	m
24 752	1556 + 1147	m
24 956	1550 + 1351	w
25 151	1550 + 1546	s

[a] s = strong, m = medium, w = weak.

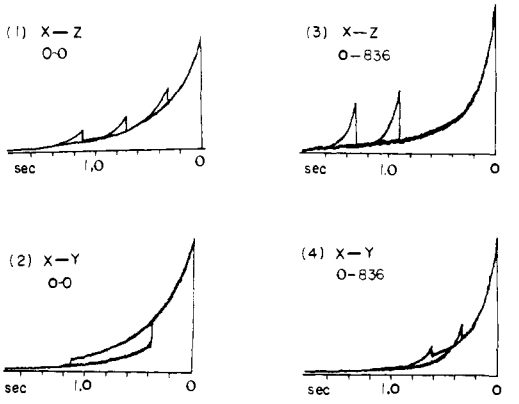

Figure 5. Decay and MIDP signals of coumarin in durene. In (1) and (2) phosphorescence signal was monitored at the 0-0 band and in (3) and (4) it was monitored at the 0-836 cm^{-1} band. One division of the horizontal scale is 0.2 s. MIDP signals were obtained by sweeping microwave at 4.2 GHz ($x \leftrightarrow z$ transition) in (1) and (3) and at 2.5 GHz ($x \leftrightarrow y$ transition) in (2) and (4).

Table III. Magnetic and Dynamic Properties of the T_1 State of Coumarin

		k_i, s^{-1}				k_i^r (relative)			p_i (relative)		
	ZFS, cm^{-1}	x	y	z	ν, cm^{-1}	x	y	z	x	y	z
Coumarin in durene	$D = 0.0980$ $E = -0.0414$	9.7	2.0	0.32	0-0 0-836 0-1628	1 1 1	4 0.25 2	0.1 0.05 0.095	1	0.29	0.05
Courmarin trap	$D = 0.0991$ $E = -0.0427$	8.7	1.8	0.28							
Coumarin in DBB	$D = 0.1001$ $E = -0.0425$	36.4	4.53	1.63	0-0	1	0.12	0.012	1	0.053	0.11

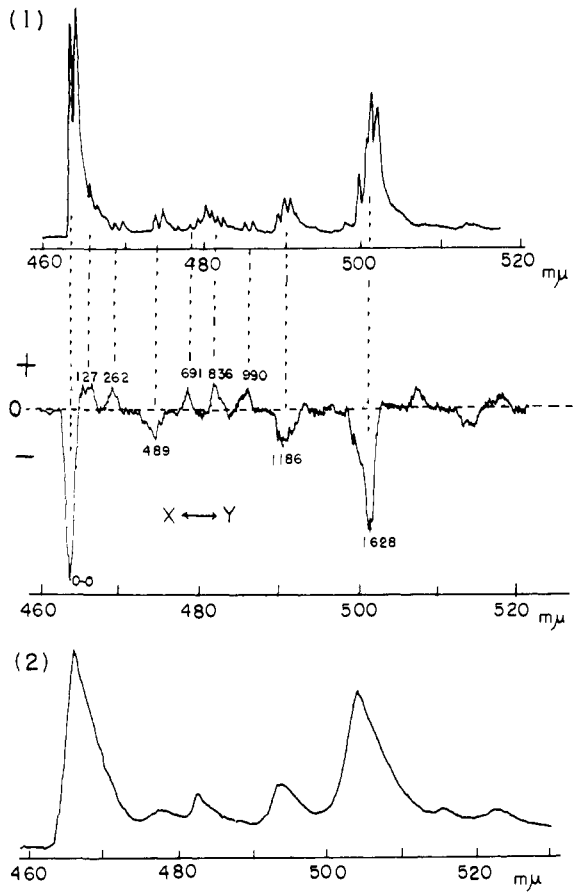

Figure 6. (1) Top: phosphorescence spectrum of coumarin in durene. Bottom: microwave modulated phosphorescence spectrum of coumarin in durene. Slit was widened in taking the bottom spectrum. + and − indicate the increase and decrease of the phosphorescence by the microwave transition at 2.5 GHz. (2) Phosphorescence spectrum of coumarin in DBB host.

considered as the a″ out-of-plane vibrations. The spectrum show $(k_x^r - k_y^r) \simeq 0$ at the 0-766 cm^{-1} bands, but this may be due to the overlap of the 0-691 and 0-836 cm^{-1} bands. It appears that the 766 cm^{-1} vibration is not an a″ vibration. Song et al. considered that the 0-737 cm^{-1} band in the low-resolution phosphorescence spectrum is due to the C-H out-of-plane mode of the pyrone moiety on the basis of polarization studies.[8] However, the relatively positive polarization of this band may be due to the superposition of the unresolved 0-691 and 0-836 cm^{-1} bands. We think that these bands are the C-H out-of-plane mode of the pyrone moiety. Our results on the vibronic level dependence of k_i^r are generally consistent with the out-of-plane polarization of the 0-0 and 0-1628 bands and relatively more in plane polarization of some other vibrational bands of the phosphorescence spectra.[5,8]

The spectra given in Figure 6 clearly show that more than 70% of the total phosphorescence emission comes from the y spin sublevel. This is remarkably different from the cases of other $^3\pi\pi^*$ aromatic carbonyls studied so far in which the z sublevel emission dominates. However, we have found $k_x \gg k_y, k_z$ as in the case of other $^3\pi\pi^*$ aromatic carbonyls. Then, our results clearly show that the decay of coumarin is dominantly radiationless and the radiationless decay predominantly originates from the x sublevel although the radiative decay is dominantly from the y sublevel. The average of k_x, k_y, and k_z gives 4.0 s^{-1}. This is somewhat larger than $k = 2.2$ s^{-1} determined by Song and Gordon in ethanol glass at 77 K.[5]

The phosphorescence spectrum of coumarin in DBB host is rather similar to that in durene host, although the spectrum is broad. The vibronic bands primarily consist of a′ vibrations, although the emission predominantly comes from the x spin sublevel throughout the entire spectrum. Hence the external heavy-atom effect in this system dominantly enhances the x sublevel emissions at the a′ vibrations.

IV. Discussions

1. Magnetic Properties. Since energy separation between the $^3\pi\pi^*$ and $^3n\pi^*$ states (ΔE_{TT}) is very large, ZFS is determined almost exclusively by spin-spin interaction. The relatively large value of $|E|$ (= 0.0425 cm^{-1}) is similar to the cases of the other systems having the ethylenic -C=C- group such as indene, indole, and benzofuran[19] and is likely due to the large spin density in the -C=C- group of the pyrone moiety

Using $A_z = 23.5$ G the z axis hfsc assigned in III.1. leads to the spin densities 0.34, 0.21 (2), and 0.17 (normalized to 1). The hfsc's of the x and y axis spectra also give similar values. Although we cannot make an unambiguous assignment of the spin densities, we make a tentative assignment based on the results of calculation by Song and Gordon[5] and our previous results on the spin density studies on indole and substituted benzenes with strongly interacting substituents.[19,41] The protons which give large splittings are expected to be those at 2, 3, 5, and 7 positions. The largest spin density is likely to be at carbon 2. In the x-axis spectrum the hfsc due to 0.15 spin density most deviates from the predicted values based on the simple model discussed in section III.1. This deviation may be primarily due to the interaction with the large spin density on the next neighbor carbon atom. If so, 0.15 spin density should be on carbon 3. Spin densities of 0.21 are then assigned to carbons 5 and 7. The present estimate places about 0.5 spin density on the -C=C- group of the pyrone moiety. Even including the uncertainties involved in the assignment of the spin densities, the spin density in the pyrone -C=C- is not likely to exceed 0.58. Song and Gordon's calculation estimates about 0.7 spin density on the pyrone -C=C- group. Their result seems to overestimate the spin density on the pyrone -C=C- group considerably.

2. Radiative and Nonradiative Properties. When the x and y axes are parallel and perpendicular to the C=O direction

and the one-center spin-orbit coupling matrix elements involving the oxygen atomic orbital are dominant in determining decay, the radiative and nonradiative decay processes are likely to be governed mainly by the local C_{2v} symmetry of the carbonyl moiety. As discussed in section III.1, the x and y axes are nearly parallel and perpendicular to the C=O direction and the analysis based on the local symmetry appears to be good in coumarin as in the cases of numerous other $^3\pi\pi^*$ aromatic carbonyls.[10,12] The relatively large radiationless decay rate from the x sublevel follows the general decay pattern of the $^3\pi\pi^*$ aromatic carbonyls with large $^3n\pi^*$ and $^3\pi\pi^*$ separation.[12] As in the other systems the spin-orbit mixing with the $^1n\pi^*$ state is considered as the primary cause of this decay.[27] However, k_x is rather small compared with the other $^3\pi\pi^*$ carbonyls because of the large energy separation between the $^3\pi\pi^*$ and $^1n\pi^*$ states ($\Delta E_{ST} \gtrsim 6200\ cm^{-1}$).

Because of the large ΔE_{TT} and ΔE_{ST} the emission from the x sublevel is also weak. The cause of the weak x sublevel emission is likely to be the vibronic spin-orbit scheme involving a'' vibrations as in the cases of many $^3\pi\pi^*$ aromatic carbonyls.[12,42-45]

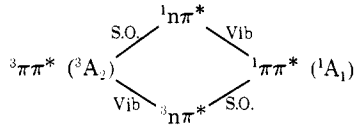

The emission of the y sublevel is due to the direct mechanism and is likely due to the spin-orbit coupling with the $^1\sigma\pi^*$ ($^1\pi\sigma^*$) state.[10,12,46] The dominance of the y sublevel emission shows that the main source of the phosphorescence emission of coumarin is due to the spin-orbit mixing with the $^1\sigma\pi^*$ ($^1\pi\sigma^*$) state rather than the $^1n\pi^*$ state. This conclusion is different from the previous suggestion that the $^1n\pi^*$ state mixing is mainly responsible for emission.[5] Our result is, however, in agreement with the results of calculation by Tanimoto et al. that the mixing with the $^1\sigma\pi^*$ ($^1\pi\sigma^*$) state is more effective than that with the $^1n\pi^*$ state in producing the radiative decay of some $^3\pi\pi^*$ aromatic carbonyls.[46]

It was found that the populating rate p_x is only three times as large as the rate p_y. This is quite different from the case of many other $^3\pi\pi^*$ aromatic carbonyls in which $p_x \gg p_y$.[10,12]

The small values of total and radiative decay rates from the z sublevel are similar to those of the other planar $^3\pi\pi^*$ molecules.[47,48]

3. External Heavy-Atom Effect in DBB Host. Enhancement of the radiative decay at the a' vibronic bands is in agreement with the results obtained by Giachino and Kearns[49] and Gash and Colson.[50] However, enhancement was made predominantly in the x sublevel emission rather than in the y sublevel emission. Therefore, the external heavy-atom effect must have introduced a new route of spin-orbit coupling rather than merely enhancing the mechanism dominant in the isolated coumarin molecule.

Acknowledgment. This work was supported in parts by a NSF institutional science development grant.

References and Notes

(1) G. S. Hammond, C. A. Stout, and A. A. Lamola, *J. Am. Chem. Soc.*, **86**, 3103 (1964).
(2) C. H. Kranch, D. M. Kramer, and A. Wacher, *Photochem. Photobiol.*, **6**, 341 (1967).
(3) L. Musajo, *Ann. Ist. Super. Sanita*, **5**, 376 (1969).
(4) P. S. Song, M. L. Harter, T. A. Moore, and W. C. Herdon, *Photochem. Photobiol.*, **14**, 521 (1971).
(5) P. S. Song and W. H. Gordon, *J. Phys. Chem.*, **74**, 4234 (1970).
(6) E. Davin, C. Balny, and R. Guglielmetta, *C. R. Hebd. Seances Acad. Sci., Ser. C*, **275**, 79 (1972).
(7) B. S. Kirkiacharian, R. Santus, and C. Helene, *Photochem. Photobiol.*, **16**, 455 (1972).
(8) W. W. Mantulin and P. S. Song, *J. Am. Chem. Soc.*, **95**, 5122 (1973).
(9) L. Goodman and M. Koyanagi, *Mol. Photochem.*, **4**, 369 (1972).
(10) T. H. Cheng and N. Hirota, *Mol. Phys.*, **27**, 281 (1974).
(11) H. Hayashi and S. Nagakura, *Mol. Phys.*, **27**, 969 (1974).
(12) E. T. Harrigan and N. Hirota, *Mol. Phys.*, **31**, 663, 681 (1976).
(13) C. R. Jones, D. R. Kearns, and R. Wing, *J. Chem. Phys.*, **58**, 1370 (1973).
(14) C. R. Jones, D. R. Kearns, and A. H. Maki, *J. Chem. Phys.*, **59**, 873 (1973).
(15) D. R. Graber, M. M. Grimes, and A. Huag, *J. Chem. Phys.*, **50**, 1623 (1969).
(16) E. T. Harrigan and N. Hirota, *Chem. Phys. Lett.*, **27**, 405 (1974).
(17) E. T. Harrigan and N. Hirota, *Chem. Phys. Lett.*, **22**, 29 (1973).
(18) S. W. Mao and N. Hirota, *Mol. Phys.*, **27**, 309 (1974).
(19) E. T. Harrigan and N. Hirota, *J. Am. Chem. Soc.*, **97**, 6647 (1975).
(20) C. A. Hutchison and B. W. Mangum, *J. Chem. Phys.*, **34**, 908 (1961).
(21) T. H. Cheng and N. Hirota, *J. Chem. Phys.*, **56**, 5019 (1972).
(22) W. Rothman, A. Case, and D. R. Kearns, *J. Chem. Phys.*, **43**, 1067 (1965).
(23) N. Hirota, *J. Chem. Phys.*, **44**, 2199 (1966).
(24) J. Schmidt, D. A. Antheunis, and J. H. van der Waals, *Mol. Phys.*, **22**, 1 (1971).
(25) J. Schmidt, Thesis, Leiden, 1972.
(26) M. A. El-Sayed, D. V. Owens, and D. S. Tinti, *Chem. Phys. Lett.*, **6**, 395 (1970).
(27) C. R. Chen and M. A. El-Sayed, *Chem. Phys. Lett.*, **10**, 307 (1971).
(28) A. H. Francis and C. B. Harris, *J. Chem. Phys.*, **57**, 1050 (1972).
(29) J. Zuclich, D. Schweitzer, and A. H. Maki, *Photochem. Photobiol.*, **18**, 161 (1973).
(30) C. A. Hutchison, "The Triplet State", A. Zahlan, Ed., Cambridge University Press, New York, N.Y., 1967, p 63.
(31) S. Bezzi and U. Croatto, *Gazz. Chim. Gel.*, **72**, 318 (1942).
(32) In the previous papers on the aromatic carbonyls, we have used an axis system in which z axis is taken along the C=O direction and the x axis is perpendicular to the molecular plane. In this paper we take the z axis perpendicular to the molecular plane in accordance with the system adapted in most papers on the EPR studies of the $\pi\pi^*$ molecules.
(33) S. P. McGlynn, T. Azumi, and M. Kinoshita, "Molecular Spectroscopy of Triplet States", Prentice-Hall, Engelwood Cliffs, N.J., 1967.
(34) A. Carrington and A. D. McLachlan "Introduction to Magnetic Resonance" Harper Row, New York, N.Y., 1967, Chapter 7.
(35) N. Hirota, C. A. Hutchison, and P. P. Palmer, *J. Chem. Phys.*, **40**, 3717 (1964).
(36) J. Zuclich, *J. Chem. Phys.*, **52**, 3592 (1970).
(37) G. Fisher, *Mol. Cryst.*, 11, 85 (1970).
(38) E. T. Harrigan and N. Hirota, unpublished observation.
(39) R. N. Jones, C. L. Angell, T. Ito, and R. J. D. Smith, *Can. J. Chem.*, **27**, 2007 (1959).
(40) P. Passigana and C. Cogrossi, *Tetrahedron*, **20**, 2859 (1964).
(41) N. Hirota, T. C. Wong, and E. T. Harrigan, *Mol. Phys.*, **29**, 903 (1975).
(42) R. M. Hochstrasser, "Molecular Aspects of Symmetry", W. A. Benjamin, New York, N.Y., 1966.
(43) W. A. Case and D. R. Kearns, *J. Chem. Phys.*, **52**, 2175 (1970).
(44) L. Goodman and M. Koyanagi, *Mol. Photochem.*, **4**, 369 (1972).
(45) Y. H. Li and E. C. Lim, *Chem. Phys. Lett.*, **7**, 15 (1970).
(46) Y. Tanimoto, H. Kobayashi, S. Nagakura, and T. Azumi, *Chem. Phys. Lett.*, **16**, 10 (1972).
(47) M. Schwoerer and H. Sixl, *Z. Naturforsch., A*, **24**, 952 (1969).
(48) D. A. Antheunis, J. Schmidt, and J. H. van der Waals, *Mol. Phys.*, **27**, 1571 (1974).
(49) G. G. Giachino and D. R. Kearns, *J. Chem. Phys.*, **53**, 3886 (1970).
(50) B. W. Gash and S. D. Colson, *J. Chem. Phys.*, **59**, 3528 (1973).